Sequential Bond Dissociation Energies of $M^+(NH_3)_x$ ($x = 1-4$) for M = Ti−Cu

Derek Walter and P. B. Armentrout*

Contribution from the Department of Chemistry, University of Utah, Salt Lake City, Utah 84112

Received September 11, 1997

Abstract: The sequential bond dissociation energies (BDEs) for $M^+(NH_3)_x$ ($x = 1-4$) for M = Ti−Cu are determined by examining the collision-induced dissociation reactions with xenon in a guided ion beam mass spectrometer. In the cases of Fe, Co, Ni, and Cu, the BDE for the second ammonia molecule is determined to be greater than the BDE for the first ammonia molecule. For all metal ions but Ti^+, the BDEs for the first two ammonia molecules are large in comparison to the BDEs for the third and fourth ammonia molecules. In general, the results of this study for the BDEs of the first and second ammonia molecules agree well with the results of previous experimental and theoretical studies. Previous studies are available only for $M^+(NH_3)_3$ (M = V, Mn, Ni, and Cu) and $M^+(NH_3)_4$ (M = V and Cu) complexes, such that this study provides the first determination of all other $(NH_3)_2M^+-NH_3$ and $(NH_3)_3M^+-NH_3$ BDEs. The trends in BDEs are discussed in terms of hybridization, dative interactions, and spin changes and compared to trends for other comprehensively studied ligands, H_2O and CO.

Introduction

A number of studies on transition metal ions solvated by small ligands have been carried out to obtain information about electronic structure and bonding effects in transition metal complexes.[1−15] In almost all of these studies, the strategy has been to analyze the trends in metal−ligand binding energies resulting from variation of the transition metal center, the ligand, and the number of ligands. These types of experiments have made it clear that a complete picture of bonding in transition metals is obtained only by considering much more than simple electrostatic effects. Such effects include the energetic cost of promoting the metal center to the bonding state, metal−ligand repulsion, and dative interactions. Ammonia, which is known to bind strongly to transition metals, is an excellent choice of ligand to extend the previous studies. Ammonia is a prototypical σ donor and does not engage in π bonding. This being the case, one may be able to obtain qualitative information about the effects of π bonding in transition metal−ligand systems by comparing ammonia ligation with other ligand systems. Another interesting property of ammonia discussed by Langhoff et al.[4] concerns the effective position of the ammonia dipole moment relative to the transition metal center in a metal ion−ligand complex, e.g. 0.48 Å closer than the effective position of the water dipole moment. This makes ammonia a strong field ligand, which provides a good opportunity to examine electronic effects that take place at the transition metal center such as hybridization and spin changes.

In addition to probing questions regarding electronic structure, $M^+(NH_3)_x$ molecules are ideal systems for studying fundamental questions related to solvation. Because of its strong hydrogen bonding capabilities, ammonia is a potent solvent with solvation properties similar to those of water. By determining the sequential metal−ammonia bond dissociation energies (BDEs) in $M^+(NH_3)_x$ molecules, one obtains information about the interactions of individual solvent molecules with the solute. Such studies are a first step in understanding liquid-phase solvation.

There have been a few investigations of $M^+(NH_3)_x$ molecules where M is a first-row transition metal. To our knowledge, two experimental and two theoretical studies exist. Holland and Castleman (HC)[10] used equilibrium methods to determine $(NH_3)_2Cu^+-NH_3$, $(NH_3)_3Cu^+-NH_3$, and $(NH_3)_4Cu^+-NH_3$ BDEs of 58.6, 53.6, and 53.6 kJ/mol, respectively, at 298 K. Collision-induced dissociation (CID) experiments were carried out by Marinelli and Squires (MS)[5] to determine M^+-NH_3 and $(NH_3)M^+-NH_3$ BDEs for M = V−Ni. Of particular interest

(1) Armentrout, P. B.; Kickel, B. L. In *Organometallic Ion Chemistry*; Kluwer Academic Publishers: Dordrecht, The Netherlands, 1996.
(2) Armentrout, P. B. *Acc. Chem. Res.* **1995**, *28*, 430.
(3) Dalleska, N. F.; Honma, K.; Sunderlin, L. S.; Armentrout, P. B. *J. Am. Chem. Soc.* **1994**, *116*, 3519.
(4) Langhoff, S. R.; Bauschlicher, C. W.; Partridge, H.; Sodupe, M. *J. Phys. Chem.* **1991**, *95*, 10677.
(5) Marinelli, P. J.; Squires, R. R. *J. Am. Chem. Soc.* **1989,** *111*, 4101.
(6) . Rosi, M.; Bauschlicher, C. W. *J. Chem. Phys.* **1989**, *90*, 7264. Rosi, M.; Bauschlicher, C. W. *J. Chem. Phys.* **1990**, *92*, 1876.
(7) Barnes, L. A.; Rosi, M.; Bauschlicher, C. W. *J. Chem. Phys.* **1990**, *93*, 609.
(8) Kemper, P. R.; Bushnell, J.; van Koppen, P.; Bowers, M. T., *J. Phys. Chem.* **1993**, *97*, 1810. Bushnell, J. E.; Maitre, P.; Kemper, P. R.; Bowers, M. T. *J. Chem. Phys.* **1997**, *106*, 10153. Kemper, P. R.; Weis, P.; Bowers, M. T. *Int. J. Mass Spectrom. Ion Processes* **1997**, *160*, 17. Weis, P.; Kemper, P. R.; Bowers, M. T. *J. Phys. Chem. A* **1997**, *101*, 2809. Bushnell, J. E.; Kemper, P. R.; Bowers, M. T. *J. Phys. Chem.* **1995**, *99*, 15602. Kemper, P. R.; Bushnell, J. E.; Maitre, P.; Bowers, M. T. *Chem. Phys. Lett.* **1995**, *242*, 244. Bushnell, J. E.; Kemper, P. R.; Bowers, M. T. *J. Phys. Chem.* **1994**, *98*, 2044. Bushnell, J. E.; Kemper, P. R.; Bowers, M. T. *J. Phys. Chem.* **1993**, *97*, 11628.
(9) Perry, J. K.; Ohanessian, G.; Goddard, W. A., *J. Phys. Chem.* **1993**, *97*, 5238.
(10) Holland, P. M.; Castleman, A. W. *J. Chem. Phys.* **1982**, *76*, 4195.
(11) Bauschlicher, C. W.; Partridge, H.; Langhoff, S. R. *J. Phys. Chem.* **1992**, *96*, 2475. Maitre, P.; Bauschlicher, C. W. *J. Phys. Chem.* **1993**, *97*, 11912.
(12) Bauschlicher, C. W.; Langhoff, S. R.; Partridge, H. *J. Chem. Phys.* **1991**, *94*, 2068.
(13) Magnera, T. F.; David, D. E.; Michl, J. *J. Am. Chem. Soc.* **1989**, *111*, 4100.
(14) Bengali, A. A.; Casey, S. M.; Cheng, C.-L.; Dick, J. P.; Fenn, P. T.; Villalta, P. W.; Leopold, D. G. *J. Am. Chem. Soc.* **1992**, *114*, 5257.
(15) Engelking, P. C.; Lineberger, W. C. *J. Am. Chem. Soc.* **1979**, *101*, 5569.

S0002-7863(97)03202-2 CCC: $15.00
Published on Web 03/19/1998

in this work was the observation that the $(NH_3)M^+-NH_3$ BDE was greater than the M^+-NH_3 BDE for M = Cr, Fe, Co, and Ni, in contrast to expectations based on simple electrostatic solvation ideas. MS also measured the $(NH_3)_2M^+-NH_3$ BDEs for M = V, Mn, and Ni and the $(NH_3)_3V^+-NH_3$ BDE.

Ab initio calculations were first carried out by Bauschlicher, Langhoff, and Partridge (BLP) on $Cu^+(NH_3)_x$ ($x = 1-4$).[12] This work is the only theoretical study that considers triply or quadruply ligated ammonia complexes of first-row transition metal ions. Theoretical calculations were also carried out by Langhoff, Bauschlicher, Partridge, and Sodupe (LBPS)[4] to determine the M^+-NH_3 and $(NH_3)M^+-NH_3$ binding energies for M = Sc−Cu. In that study, LBPS determined that both the $(NH_3)M^+-NH_3$ BDE and M^+-NH_3 BDEs were roughly 160−200 kJ/mol. In addition, it was determined that the $(NH_3)M^+-NH_3$ BDE was greater than the M^+-NH_3 BDE for M = Cr, Fe, and Co, but not Ni, in contrast to the results of MS.[5] These calculations show that this result is attributable to favorable 4s−3d σ hybridization that removes metal−ligand repulsion along the bonding axis. Overall, the results of LBPS show good agreement with the results of MS,[5] although V and Co complexes were singled out as showing large discrepancies.

In this study, we report the sequential BDEs at 0 K for $M^+(NH_3)_x$ ($x = 1-4$) for M = Ti−Cu. These are determined by analysis of the kinetic energy dependence of the CID reactions of these complexes with xenon in a guided ion beam mass spectrometer. The data analysis includes consideration of multiple ion−neutral collisions, the internal energies of the complexes, and the dissociation lifetimes. The results of this study are compared with the previous theoretical and experimental results and interpreted in terms of both electrostatics and electronic effects that are unique to the transition metals. The periodic trends in these values are then compared with those of other first-row transition metal ion complexes involving H_2O and CO.

Experimental Methods

General. All experiments were performed using a guided ion beam mass spectrometer described in detail elsewhere.[16] Briefly, ions are formed, extracted from the source, accelerated, and focused into a magnetic sector momentum analyzer for mass analysis. Mass-selected ions are then slowed to a desired kinetic energy and focused into an radio frequency (rf) octopole ion beam guide that traps the ions radially. The octopole passes through a static gas cell containing the collision gas xenon. The xenon gas pressure is kept low (<0.30 mTorr) so that multiple collisions are improbable, and the pressure dependence of the reaction probability is explicitly examined (see below). After exiting the gas cell, product and unreacted parent ions drift to the end of the octopole where they are focused into a quadrupole mass filter for mass analysis. The ions are detected by a secondary electron scintillation detector. Ion intensities are converted to absolute cross sections as described previously.[16] Absolute uncertainties in cross section magnitudes are estimated to be ±20%.

The energy of motion of the center-of-mass of two reacting species through the laboratory cannot help drive a chemical reaction as this energy is conserved throughout the reaction. All laboratory energies are therefore converted to center-of-mass energies using the expression $E(\mathrm{CM}) = E(\mathrm{lab})\, m/(m + M)$, where M and m are the masses of the ion and neutral reactants, respectively. All energies stated in this paper are in the center-of-mass frame unless otherwise noted. To determine the absolute zero and distribution of the ion beam kinetic energy, the octopole is used as a retarding energy analyzer.[16] The uncertainty in the absolute energy scale is ±0.05 eV in the laboratory frame. The full widths at half-maximum (fwhm) of the ion energy distributions range from 0.2 to 0.6 eV (lab).

Ion Source. The ion source used here is a 1-m direct current (dc) discharge/flow tube source[17] operating at a pressure of 0.5−0.7 Torr. At the front end of the flow tube is a cathode held at a potential of 1.5−2.5 kV in a flow of 5−15% argon in helium. The cathode is constructed from the metal of interest except for Mn, where chunks of the metal are held in a Ta boat. Ions are generated in a continuous discharge by argon ion sputtering of the metal cathode. Transition metal−NH_3 clusters are formed by associative reactions with NH_3 gas introduced 50 cm downstream from the discharge at a pressure of roughly 40 mTorr.

The flow conditions used in this source provide $>10^4$ collisions between an ion and the buffer gas, which should thermalize the ions both rotationally and vibrationally. We assume that the clusters formed in this study are in their ground electronic states and that the internal energy is well described by a Maxwell−Boltzmann distribution at 298 K. Previous work from this laboratory has shown these assumptions to be reasonable.[18,19]

In the case of Cr^+ complexes, there is an isobaric interference from protonated ammonia clusters, i.e. the major isotope of Cr^+ at 52 m/z has the same nominal mass as $(NH_3)_3H^+$. Although high pressures of ammonia in the flow tube would generate $(NH_3)_xH^+$ clusters as the dominant species, sufficiently low pressures could be found that no such contaminants complicated the CID spectrum of $Cr^+(NH_3)_x$ complexes. This was verified by high-energy CID spectra and by examining the energy dependence for loss of one ammonia molecule. The proton-bound clusters, $(NH_3)_{x+3}H^+$, have weaker binding energies than the isobaric $Cr^+(NH_3)_x$ complexes and were therefore readily observed.

Thermochemical Analysis. To account for the effects of multiple reactant ion collisions with xenon, the experiments were performed at two different pressures of Xe, typically ≈0.2 and ≈0.1 mTorr. If a particular cross section was observed to vary with pressure, it was linearly extrapolated to zero pressure by a method described previously.[20] This provides cross sections attributable only to a single ion−Xe collision. In all cases, the cross sections showed little or no pressure dependence so extrapolation was usually unnecessary. However, for $Co^+(NH_3)_2$, $Ni^+(NH_3)_2$, and $Cu^+(NH_3)_2$, the pressure dependence was great enough to warrant an extrapolation. This is largely a consequence of these complexes having the strongest bond energies (see below).

The cross sections were then modeled in the threshold region with eq 1, where σ_0 is an energy-independent scaling parameter, E is the

$$\sigma(E) = \sigma_0 \sum g_i (E + E_{\mathrm{rot}} + E_i - E_0)^n / E \qquad (1)$$

relative translational energy of the reactants, E_{rot} is the rotational energy of the reactants ($3kT/2$ for all complexes studied here), E_0 is the threshold for reaction of the ground vibrational and electronic state, and n is an adjustable parameter. The summation is over i which denotes the vibrational states of the cluster ions, g_i is the population of those states ($\sum g_i = 1$), and E_i is the excitation energy of each vibrational state. With n taken to be equal to 1, this equation can be recognized as a variation on the line-of-centers model for reaction cross sections that takes explicit account of the internal energy of the reactant ion. Because the cluster ions of interest in this study have many low-frequency vibrational modes, the populations of excited vibrational modes are not negligible even at 298 K. Thus, the internal energy of the reactant ion contributes significantly to the reaction threshold. The Beyer−Swinehart algorithm[21] is used to calculate the distribution of vibrational energies at 298 K from the vibrational frequencies. The values for vibrational frequencies are chosen as described below.

(16) Ervin, K. M.; Armentrout, P. B. *J. Chem. Phys.* **1985**, *83*, 166.

(17) Schultz, R. H.; Armentrout, P. B. *Int. J. Mass Spectrom. Ion Processes* **1991**, *107*, 29

(18) Schultz, R. H.; Armentrout, P. B. *J. Chem. Phys.* **1992**, *96*, 1046. Schultz, R. H.; Crellin, K. C.; Armentrout, P. B. *J. Am. Chem. Soc.* **1991**, *113*, 8590. Fisher, E. R.; Kickel, B. L.; Armentrout, P. B. *J. Phys. Chem.* **1993**, *97*, 10204. Fisher, E. R.; Kickel, B. L.; Armentrout, P. B. *J. Chem. Phys.* **1992**, *97*, 4859.

(19) Khan, F. A.; Clemmer, D. C.; Schultz, R. H.; Armentrout, P. B. *J. Phys. Chem.* **1993**, *97*, 7978.

(20) Hales, D. A.; Lian, L.; Armentrout, P. B. *Int. J. Mass Spectrom. Ion Processes* **1990**, *102*, 269.

At higher energies, the cross sections are modeled with a modified form of eq 1 that accounts for a decline in a particular product ion cross section due to further dissociation. The model that reproduces this behavior has been described previously and depends on E_D, the energy where the loss of a second NH_3 ligand can begin, and p, a parameter similar to n in eq 1.[22] Before comparison with the data, the model cross section of eq 1 is convoluted with the kinetic energy distributions of the ion and neutral reactants.[16,23] The parameters in eq 1, σ_0, n, and E_0, are then optimized using a nonlinear least-squares analysis until the convoluted model cross section best reproduces the data.

Another consideration in the analysis of CID thresholds is whether dissociation of the activated cluster molecule occurs within the $\sim 10^{-4}$ s it takes for the molecule to pass from the octopole to the detector. If the lifetime of the activated complex exceeds this time frame, then the apparent thresholds will be shifted to higher energies. For large molecules, with many vibrational modes to randomize the available energy, this effect is apparent. Therefore, the data for all quadruply ligated systems was analyzed by incorporating an RRKM treatment into eq 1 as described previously.[19,24,25] Briefly, eq 1 is integrated over a dissociation probability determined from the set of rovibrational frequencies appropriate for the energized molecule and the transition state (TS) leading to dissociation. To carry out this calculation, the only information required is the rovibrational frequencies of the TS. In the case of an ion−molecule dissociation reaction, the ion and molecule interact primarily through an electrostatic ion-induced dipole potential. Thus, it is most appropriate to think of the TS leading to dissociation as a loose TS that has many vibrational frequencies that are equal to those of the products. For the loss of NH_3 from $M^+(NH_3)_4$, there are five vibrational modes that ultimately become translations and rotations in the dissociated products. These transitional modes are taken to be the five lowest values of the new frequencies introduced in going from $M^+(NH_3)_3$ to $M^+(NH_3)_4$. The sixth new frequency, one of the four nearly degenerate metal−ammonia stretching modes, is taken to be the reaction coordinate. The five transitional modes are treated as rotors in the TS, a treatment that corresponds to a phase space limit and is described in detail elsewhere.[25] Briefly, two of the rotors have rotational constants of free ammonia ($B = 6.196$ cm^{-1}),[26] those with axes perpendicular to the reaction coordinate. Another pair of rotors have rotational constants of the $M^+(NH_3)_3$ product ($B = 0.1214$ cm^{-1}), again those with axes perpendicular to the reaction coordinate. These rotational constants were calculated by treating the $M^+(NH_3)_3$ product as a pseudo-trigonal planar molecule with M^+-NH_3 bond lengths equal to the calculated Ti^+-N bond distance in $Ti^+(NH_3)$ (2.236 Å)[4] plus the distance from the nitrogen to the NH_3 center of mass (0.094 Å). Because the calculations are fairly insensitive to the magnitude of the rotational constants, this method of determining the rotational constant should be sufficient for the complexes of all metals. Of the two rotational constants of the products with axes parallel to the reaction coordinate, one is a transitional mode and is assigned as the remaining rotational constant of the NH_3 product ($B = 9.444$ cm^{-1}).[26] The other becomes an external rotation of the TS and is calculated to be 0.0607 cm^{-1} by treating the $M^+(NH_3)_3$ product as a pseudo-trigonal planar molecule. The other two external rotors of the TS are calculated using a variational treatment described elsewhere[25] which assumes that the TS is located at the centrifugal barrier for interaction of NH_3 with $M^+(NH_3)_3$. This RRKM treatment resulted in shifts of 0.0−0.12 eV depending on the system. Test calculations for triply ligated complexes indicate that the RRKM treatment lowers these thresholds by about 0.03 eV for titanium (the most strongly bound complex) and less than 0.01 eV for all other metals. Shifts for smaller complexes will be even less. Thus, the lifetime effects are not included in the results for $x = 1-3$ with the exception of $Ti^+(NH_3)_3$.

Table 1. Fe^+−Ligand Stretching and Bending Frequencies of $Fe^+(H_2O)_x$ and NH_3 Frequencies

species	vibrational frequencies (degeneracies) cm^{-1}
$Fe^+(H_2O)$[a]	312, 347, 519
$Fe^+(H_2O)_2$[a]	44, 102(2), 185(2), 369, 485, 546(2)
$Fe^+(H_2O)_3$[a]	35, 57, 90, 96, 132, 140, 270, 286, 314, 343, 362, 404, 492, 519, 534
$Fe^+(H_2O)_4$[a]	35, 49, 60, 96, 100, 124, 143, 204, 246, 266, 269, 282, 337, 348, 354, 369, 377, 443, 455, 506, 534
NH_3[b]	3337, 950, 3444(2), 1627(2)

[a] Reference 28. [b] Reference 29.

The uncertainties in the reported reaction thresholds arise from three main sources. First, uncertainty is introduced by the range of E_0 values that will acceptably reproduce the cross section data. Second, uncertainty is introduced from an estimated ±25% uncertainty in the vibrational frequencies. Finally, there is a 0.05-eV uncertainty in the laboratory energy scale. In the case of $M^+(NH_3)_4$ systems, additional uncertainty arises from variation of the RRKM parameters used to fit the data. In this study, uncertainty in the thresholds due to varying the time window for dissociation ($\sim 10^{-4}$ s) by 1/2 and 2 and the rovibrational frequencies for the TS by ±25% is included.

Because all sources of energy available to the reactants are included in this data analysis, thresholds obtained correspond to 0 K values. In the absence of reverse activation barriers to dissociation, these thresholds correspond directly to BDEs at 0 K. Reverse activation barriers are unexpected in these metal−ligand dissociation processes both because quantum mechanical considerations demonstrate that the potential energy surfaces are attractive for such heterolytic bond dissociations[27] and because of the long-range attractive ion-induced dipole and ion−dipole interactions.

Vibrational Frequencies. To our knowledge, there are no calculated frequencies for transition metal−ammonia clusters. This being the case, frequencies must be estimated. The metal−ligand frequencies were estimated using a reduced Morse potential to relate them to a set of frequencies calculated by Ricca and Bauschlicher for $Fe^+(H_2O)_x$ (Table 1).[28] The ratio of the metal−ligand frequencies for species 1 and 2, γ, is given by eq 2, where μ and D_e are the reduced mass and potential

$$\gamma = \omega_1/\omega_2 = [(D_e/m)_1/(D_e/\mu)_2]^{1/2} \quad (2)$$

energy well depths, respectively. Values for γ are found in an iterative process by fitting the data for unknown species 1 using frequencies for species 2, chosen to be similar to species 1. This provides an inital estimate of D_{e1} that is then used to scale the original frequencies using eq 2. This revised set of frequencies is then used to refit the data. The process is repeated until D_{e1} is self-consistent. Values of γ for all of the cluster molecules considered in this study are summarized in Table 2. The remaining vibrational modes for the cluster molecules are taken to be the frequencies of free ammonia. These frequencies were taken from the compilation of Shimanouchi[29] and are summarized in Table 1.

Comparison of 298 and 0 K BDEs. To compare our experimentally determined 0 K BDEs for $M^+(NH_3)_x$ to those in the literature, which are typically reported at 298 or 300 K, we must convert to 298 K values. The required information for NH_3 and the transition metal ions are taken from the JANAF Tables.[30] For the metal ammonia ions, the required enthalpy change between 0 K and a temperature T is given

(21) Beyer, T.; Swinehart, D. F. *Commun. ACM* **1973**, *16*, 379. Stein, S. E.; Rabinovitch, B. S. *J. Chem. Phys.* **1977**, *53*, 2438. Stein, S. E.; Rabinovitch, B. S. *Chem. Phys. Lett.* **1977**, *49*, 183. Gilbert, R. G.; Smith, S. C. *Theory of Unimolecular and Recombination Reactions*; Blackwell Scientific Publications: Oxford, U.K., 1990.

(22) Weber, M. E.; Elkind, J. L.; Armentrout, P. B. *J. Chem. Phys.* **1986**, *84*, 1521.

(23) Lifshitz, C.; Wu, R. L. C.; Tiernan, T. O.; Terwiliger, D. T. *J. Chem. Phys.* **1978**, *68*, 247.

(24) Loh, S.; Hales, D. A.; Lian, L.; Armentrout, P. B. *J. Chem. Phys.* **1989**, *90*, 5466.

(25) Rodgers, M. T.; Ervin, K. M.; Armentrout, P. B. *J. Chem. Phys.* **1997**, *106*, 4499.

(26) Herzberg, G. *Molecular Spectra and Molecular Structure III*; van Nostrand: New York, 1966.

(27) Armentrout, P. B.; Simons, J. *J. Am. Chem. Soc.* **1992**, *114*, 8627.

(28) Ricca, A.; Bauschlicher, C. W. *J. Phys. Chem.* **1995**, *99*, 9003.

(29) Shimanouchi, T. *Tables of Molecular Vibrational Frequencies: Consolidated Volume 1*; NSRDS-NBS 39; U.S. Government Printing Office: Washington, DC, 1972.

(30) Chase, M. W.; Davies, C. A.; Downey, J. R.; Frurip, D. J.; McDonald, R. A.; Syverud, A. N. *J. Phys. Chem. Ref. Data* **1988**, *14* (Suppl. No. 1) [JANAF tables].

Table 2. Values of γ for $M^+(NH_3)_x$ Cluster Molecules[a]

	x			
M	1	2	3	4
Ti	1.25	1.03	1.74	1.73
V	1.21	1.04	1.30	1.40
Cr	1.20	1.06	0.98	0.88
Mn	1.07	1.02	1.02	0.90
Fe	1.18	1.20	1.03	1.02
Co	1.26	1.28	1.06	1.04
Ni	1.30	1.25	1.27	0.97
Cu	1.27	1.24	0.90	0.97

[a] Calculated using eq 2.

by eq 3, where $u = h\nu_i/k_BT$. The summation in eq 3 is carried out over the vibrational frequencies of the polyatomic molecule, ν_i.

$$[H^\circ_T - H^\circ_0]_{\text{compound}} \sim 4RT + RT\sum u/(e^u - 1) \qquad (3)$$

Results

Cu^+ is the only metal where there are both experimental and theoretical determinations in the literature for the $M^+(NH_3)_x$ BDEs for $x = 1-4$. Hence, we choose to use the Cu^+ system to illustrate the general features of the kinetic energy dependent cross sections of the metal−ligand complexes. Our experimental results for all other metal systems are qualitatively similar.

For $M^+(NH_3)$, we observe only the CID product, M^+, and the ligand exchange product, M^+Xe, as formed in reactions 4 and 5.

$$M^+(NH_3) + Xe \rightarrow M^+ + NH_3 + Xe \qquad (4)$$

$$\rightarrow M^+Xe + NH_3 \qquad (5)$$

The apparent thresholds for CID with all metals examined were roughly 2 eV, and the thresholds for the ligand exchange reaction were typically 0.5−1.0 eV lower. Ligand exchange products were not observed for M = Ti because the intensity of the $Ti^+(NH_3)$ beam was too small nor for M = Mn presumably because the bond of the Mn^+Xe species should be fairly weak. Figure 1 shows the results for the CID of $Cu^+(NH_3)$. The cross section for formation of Cu^+Xe rises smoothly from a threshold of roughly 2 eV and has a maximum magnitude of about 1 Å^2 at an energy of 3 eV. At this point, the ligand exchange cross section begins to decline as the cross section for CID rises from threshold. The decline of the ligand exchange cross section with the onset of the CID cross section indicates that the two processes are in competition with one another.

For the dissociation of $M^+(NH_3)_x$ ($x > 1$), the sequential loss of NH_3 from the cluster molecules is observed for all metals examined. In some cases, the ligand exchange products, $M^+(NH_3)_{x-y}Xe$ ($y < x$), were also observed although these cross sections are quite small. For the doubly ligated species, $M^+(NH_3)_2$, the thresholds for loss of NH_3 were roughly 2 eV, similar to the apparent thresholds for loss of NH_3 from $M^+(NH_3)$. This can be seen in the data for the CID of $Cu^+(NH_3)_2$, Figure 2. Note that cross section has a maximum magnitude of about 14 Å^2, approximately twice that for $Cu^+(NH_3)$. Because the ligand exchange and CID processes are in competition with one another, the cross section for formation of $Cu^+(NH_3)Xe$ begins to decline at the onset for CID. At higher energies, both Cu^+Xe and Cu^+ are formed in small quantities. The cross section for formation of Cu^+Xe declines beginning at the onset for formation of Cu^+.

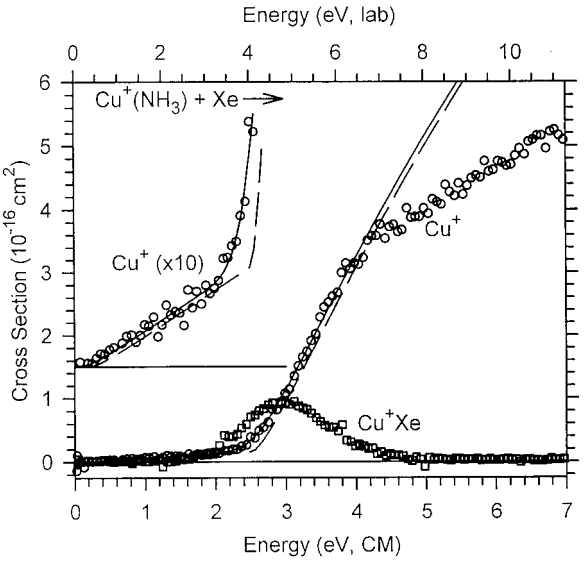

Figure 1. Cross sections for the CID of $Cu^+(NH_3)$ with Xe to form the ligand exchange product, Cu^+Xe (squares), and the CID product, Cu^+ (circles), as a function of laboratory kinetic energy (upper *x*-axis) and center-of-mass kinetic energy (lower *x*-axis). The dashed lines are the sum of the models of eq 1 for 0 K reactants for fitting the low- and high-energy regions of the cross section (see text). The solid line shows this model convoluted over the translational, vibrational, and rotational energy distributions of the reactants. Also shown is the threshold region for the CID product magnified by a factor of 10.

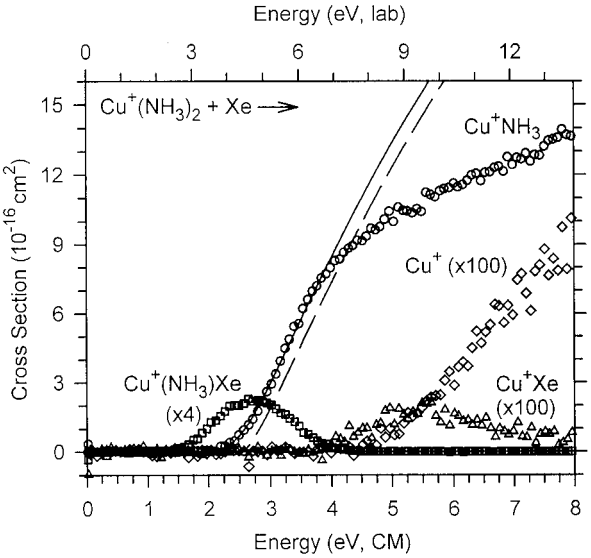

Figure 2. Cross sections for the CID of $Cu^+(NH_3)_2$ with Xe to form $Cu^+(NH_3)$ (open circles), Cu^+ (open diamonds, multiplied by a factor of 100), $Cu^+(NH_3)Xe$ (open squares, multiplied by a factor of 4), and Cu^+Xe (open triangles, multiplied by a factor of 100) as a function of laboratory kinetic energy (upper *x*-axis) and center-of-mass kinetic energy (lower *x*-axis). The dashed line is the model of eq 1 for 0 K reactants. The solid line shows this model convoluted over the translational, vibrational, and rotational energy distibutions of the reactants.

For the triply and quadruply ligated systems, the apparent thresholds for loss of a single ligand decrease to below 0.5 eV. This can be seen in the cross sections for the CID of $Cu^+(NH_3)_3$ and $Cu^+(NH_3)_4$, shown in Figures 3 and 4, respectively. Clearly, the third and fourth ammonia molecules are bound weakly compared to the first and second NH_3 ligands. The data for $Cu^+(NH_3)_4$ (Figure 4) show a rapid decline in the cross section for $Cu^+(NH_3)_3$ at about 0.6 eV. This rapid decline coincides

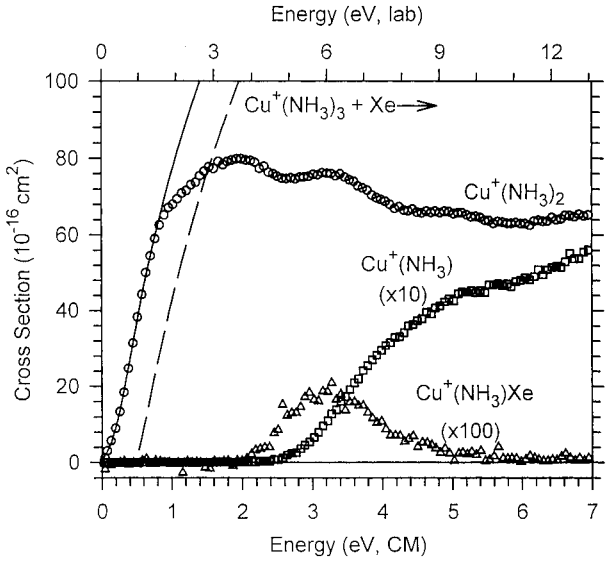

Figure 3. Cross sections for the CID of $Cu^+(NH_3)_3$ with Xe to form $Cu^+(NH_3)_2$ (open circles), $Cu^+(NH_3)$ (open squares, multiplied by a factor of 10), and $Cu^+(NH_3)Xe$ (open triangles, multiplied by a factor of 100) as a function of laboratory kinetic energy (upper *x*-axis) and center-of-mass kinetic energy (lower *x*-axis). The dashed line is the model of eq 1 for 0 K reactants. The solid line shows this model convoluted over the translational, vibrational, and rotational energy distributions of the reactants.

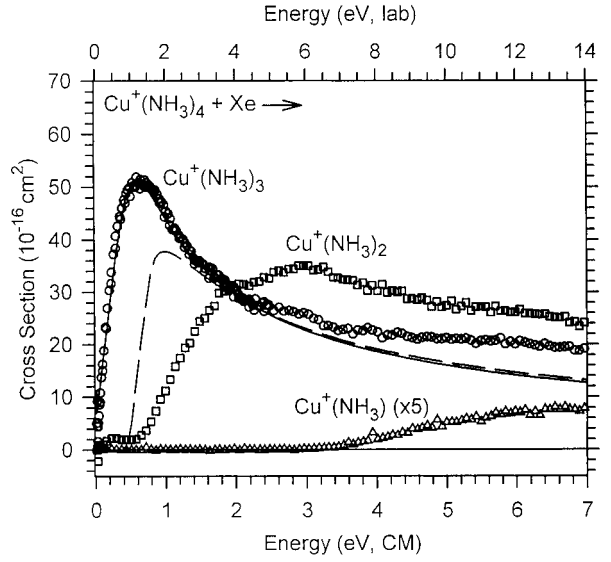

Figure 4. Cross sections for the CID of $Cu^+(NH_3)_4$ with Xe to form $Cu^+(NH_3)_3$ (open circles), $Cu^+(NH_3)_2$ (open squares), and $Cu^+(NH_3)$ (open triangles, multiplied by a factor of 5) as a function of laboratory kinetic energy (upper *x*-axis) and center-of-mass kinetic energy (lower *x*-axis). The dashed line is the model of eq 1 for 0 K reactants. The solid line shows this model convoluted over the translational, vibrational, and rotational energy distributions of the reactants.

with the rise of the cross section for loss of two ammonia ligands, indicating that the dissociations are clearly sequential. Such rapid declines in the cross sections are not observed for the triply or doubly ligated system because the BDEs for loss of ammonia from $Cu^+(NH_3)_2$ and $Cu^+(NH_3)$ are high relative to the BDEs for loss of ammonia from $Cu^+(NH_3)_3$ and $Cu^+(NH_3)_4$.

The early first-row transition metal ions (Sc^+-V^+) have been observed to react exothermically with NH_3 to form H_2 and MNH^+.[31] Consistent with this, we note that $MNH^+(NH_3)_x$ clusters were abundantly formed in the flow tube source for M = Ti. We therefore checked to see if any $MNH^+(NH_3)_{x-1}$ products were formed upon collisional excitation of $M^+(NH_3)_x$ complexes with Xe. In the case of $x = 1$, such products could be formed endothermically from the $M(NH_3)^+$ species with thermodynamic thresholds of 1.37 ± 0.14 eV for Ti and 1.84 ± 0.20 eV for V.[31] These thresholds would lie 0.65 and 0.12 eV, respectively, below the thresholds measured for simple CID. No such products were observed for any metals, although the sensitivity to such products is not extremely high because of overlap with the much more intense reactant ion beam. Given the limited sensitivity to these products and the previous observation that the electronic ground states of Ti^+ and V^+ react quite inefficiently with ammonia at thermal energies (reaction efficiencies of about 10 and 1%, respectively),[31] the failure to observe such dehydrogenation species is not particularly surprising. Further, competition with the much more favorable CID process to yield intact ammonia molecules would limit the observation of dehydrogenation products to a fairly narrow range of kinetic energies.

For $Fe^+(NH_3)_2$ and $Mn^+(NH_3)_3$, the formation of NH_4^+ was observed at higher energies. In both cases, the apparent threshold was between 6 and 7 eV with maximum cross sections of only 0.05 and 0.02 Å^2, respectively, at about 10 eV. The thresholds are consistent with the thermochemistry calculated for process 6, 6.0 and 5.9 eV for the Fe and Mn complexes,

$$M^+(NH_3)_x + Xe \rightarrow M + NH_4^+ + NH_2 + (x-2)NH_3 + Xe \quad (6)$$

respectively. It seems likely that this process could be occurring for other complexes but was not observed because of the small size of the cross section.

Cross section data for all metal ion ammonia complexes was analyzed using eq 1 and the methods described above. A complicating factor in the analysis of much of the data is a low-energy feature that causes the cross section for CID to have a nonzero magnitude at low energies. An example of such a feature is obvious in the CID cross section for $Cu^+(NH_3)$ in Figure 1. This feature could be due to a small amount of excited electronic state of the metal−ligand complex that is present in the beam, although other origins cannot be ruled out. Attempts at quenching this excited state by introducing NO, O_2, and CH_4 gases into the flow tube were unsuccessful. A similar result was obtained in a study by Meyer et al.[32] on transition metal ion−benzene systems. The low-energy feature was present in many of the data sets, but its magnitude and pressure dependence varied from system to system. In a number of cases, $Ti^+(NH_3)$, $Cr^+(NH_3)$, $Mn^+(NH_3)$, $V^+(NH_3)_2$, $Cr^+(NH_3)_2$, $Cu^+(NH_3)_2$, $Cr^+(NH_3)_3$, $Co^+(NH_3)_3$, $Ni^+(NH_3)_3$, $Cu^+(NH_3)_3$, and quadruply ligated systems for Cr to Cu, the low-energy feature could be ignored without affecting the thresholds obtained. For all other systems, the low-energy feature influenced the threshold determined and the data analysis was handled as follows. First, the data were analyzed while ignoring the presence of the low-energy feature. Because the low-energy feature causes the cross sections to rise prematurely, this analysis will give a lower limit to the threshold. Second, the low-energy feature was fit using eq 1 and the fit of the low-energy feature was subtracted from

(31) Clemmer, D. E.; Sunderlin, L. S.; Armentrout, P. B. *J. Phys. Chem.* **1990**, *94*, 208. Clemmer, D. E.; Sunderlin, L. S.; Armentrout, P. B. *J. Phys. Chem.* **1990**, *94*, 3008.

(32) Meyer, F.; Khan, F. A.; Armentrout, P. B. *J. Am. Chem. Soc.* **1995**, *117*, 9740.

Table 3. Parameters of Eq 1 Used To Model Cross Sections[a]

x	M	E_0 (eV)	*n*	σ_0
1	Ti	2.02(0.07)	1.1(0.1)	1.1(0.1)
	V[b]	1.93(0.08)	1.3(0.2)	6.4(0.7)
	c	2.00(0.08)	1.2(0.2)	6.8(0.7)
	Cr	1.89(0.10)	1.1(0.1)	14.0(1.8)
	Mn	1.52(0.08)	1.2(0.2)	7.6(0.7)
	Fe[b]	1.85(0.09)	1.5(0.2)	8.4(1.1)
	c	1.94(0.08)	1.4(0.2)	9.0(0.7)
	Co[b]	2.19(0.09)	1.5(0.2)	5.2(0.7)
	c	2.33(0.11)	1.4(0.2)	6.0(0.8)
	Ni[b]	2.35(0.12)	1.5(0.2)	3.0(0.5)
	c	2.44(0.10)	1.5(0.2)	3.0(0.4)
	Cu[b]	2.39(0.10)	1.5(0.2)	6.2(1.1)
	c	2.52(0.08)	1.4(0.2)	6.8(0.9)
2	Ti[b]	1.72(0.09)	1.4(0.2)	6.9(0.9)
	c	1.91(0.08)	1.2(0.1)	7.9(0.7)
	V	1.70(0.09)	1.4(0.2)	16.9(1.9)
	Cr	1.85(0.09)	1.4(0.2)	27.2(4.2)
	Mn[b]	1.54(0.09)	1.6(0.2)	16.2(2.0)
	c	1.61(0.08)	1.5(0.2)	16.9(1.6)
	Fe[b]	2.30(0.09)	1.3(0.2)	9.8(1.3)
	c	2.37(0.07)	1.3(0.1)	10.6(0.9)
	Co[b]	2.54(0.09)	1.2(0.2)	13.4(1.6)
	c	2.59(0.09)	1.2(0.2)	7.9(0.7)
	Ni[b]	2.55(0.09)	1.1(0.2)	10.7(1.3)
	c	2.62(0.09)	1.1(0.2)	11.2(1.3)
	Cu	2.55(0.10)	1.4(0.2)	17.2(2.7)
3	Ti[b]	1.72(0.08)	1.6(0.1)	16.0(2.3)
	c	1.92(0.09)	1.4(0.2)	18.2(2.7)
	V[b]	1.04(0.08)	1.5(0.2)	32.3(3.0)
	c	1.11(0.08)	1.3(0.2)	34.6(2.4)
	Cr	0.56(0.06)	1.1(0.1)	54.0(2.1)
	Mn[b]	0.61(0.06)	1.3(0.2)	57.6(1.4)
	c	0.72(0.05)	1.1(0.1)	55.7(2.7)
	Fe[b]	0.63(0.10)	1.4(0.2)	44.1(1.0)
	c	0.77(0.06)	1.1(0.2)	42.9(3.2)
	Co	0.66(0.06)	1.4(0.1)	48.8(2.1)
	Ni	0.93(0.08)	1.5(0.2)	33.3(2.5)
	Cu	0.49(0.06)	1.4(0.1)	106.0(2.5)
4	Ti[b]	1.60(0.07)	1.3(0.2)	32.7(3.2)
	c	1.63(0.08)	1.3(0.2)	31.2(4.2)
	V[b]	0.95(0.08)	1.3(0.2)	54.8(2.1)
	c	1.01(0.07)	1.1(0.1)	56.4(1.1)
	Cr	0.31(0.09)	1.2(0.1)	75.3(10.7)
	Mn	0.37(0.06)	1.3(0.2)	95.1(18.5)
	Fe	0.44(0.07)	1.0(0.1)	84.0(2.9)
	Co	0.51(0.06)	1.0(0.1)	92.1(4.5)
	Ni	0.38(0.06)	1.4(0.1)	124.6(10.0)
	Cu	0.44(0.06)	1.3(0.1)	114.4(25.0)

[a] Uncertainties listed in parentheses. [b] Results obtained by modeling cross sections while ignoring the low-energy feature. Thresholds obtained from this method of analysis should be thought of as lower limits to the true thresholds. [c] Results obtained by modeling cross sections after subtracting out the low-energy feature. Thresholds obtained from this method of analysis should be thought of as upper limits to the true thresholds.

the cross section. This gave modified cross sections that rise smoothly from the threshold. Figure 1 shows an example of this composite fit and demonstrates that this accurately reproduces the observed cross section over an extended range of energies. It is likely that thresholds derived by analyzing these modified cross sections are closer to the true thresholds, but there is certainly ambiguity in the procedure used to model the low-energy features. Thus, the thresholds derived from analyzing the modified cross sections are most conservatively thought of as upper limits to the true threshold. In most cases (10 out of 16), the upper and lower limits to the thresholds differ by less than 0.1 eV and no cases differ by more than 0.2 eV. The parameters used to model the unmodified and modified cross sections are summarized in Table 3.

Table 4. Summary of 298 K Binding Enthalpies in kJ/mol[a]

		x				
M	source	1	2	$\Delta(2,1)$[b]	3	4
Ti	this study[c]	197(7)	176(17)	−21(18)	184(18)	161(9)
	LBPS[d]	187(13)	158(13)	−29(18)		
V	this study[c]	192(11)	164(9)	−28(14)	109(11)	99(10)
	MS[e]	217(19)	188(19)	−29(27)	94	78
	LBPS[d]	184(13)	169(13)	−15(18)		
Cr	this study[c]	183(10)	179(9)	−4(13)	54(6)	30(9)
	MS[e]	157(19)	171(19)	14(27)		
	LBPS[d]	163(13)	171(13)	8(18)		
Mn	this study[c]	147(8)	153(12)	6(14)	66(10)	36(6)
	MS[e]	154(19)	143(19)	−11(27)	49	
	LBPS[d]	148(13)	118(13)	−30(18)		
Fe	this study[c]	184(12)	227(11)	43(16)	69(15)	44(7)
	MS[e]	161(19)	204(19)	43(27)		
	LBPS[d]	180(13)	212(13)	32(18)		
Co	this study[c]	219(16)	250(11)	31(19)	65(6)	51(6)
	MS[e]	246(19)	255(19)	9(27)		
	LBPS[d]	211(13)	219(13)	8(18)		
Ni	this study[c]	238(19)	251(12)	13(22)	93(8)	35(6)
	MS[e]	214(19)	230(19)	16(27)	74	
	LBPS[d]	235(13)	211(13)	−24(18)		
Cu	this study[c]	237(15)	248(10)	11(18)	46(6)	45(6)
	LBPS[d]	216(13)	218(13)	2(18)		
	BLP[f]	224(13)	225(13)	1(18)	71(13)	54(13)
	HC[g]				59(1)	54(1)

[a] Uncertainties in parentheses. [b] $D[(NH_3)M^+-NH_3] - D(M^+-NH_3)$. [c] Average of upper and lower limit values for binding enthalpies (see text) with uncertainties that represent the dispersion in these values and their uncertainties. [d] Results of Langhoff et al. converted to 298 K.[4] [e] Results of Marinelli and Squires.[5] These results are taken to be 298 K values. [f] Results of Bauschlicher et al. converted to 298 K.[12] [g] 298 K results of Holland and Castleman.[10]

Discussion

The average of the thresholds listed in Table 3 are converted to 298 K binding enthalpies using eq 3. Uncertainties in values obtained with and without explicit modeling of the low-energy feature include the dispersion in the two values for each system and the uncertainties in the individual threshold values. These binding enthalpies are summarized in Table 4 along with 298 K binding enthalpies of previous experimental and theoretical results. BDEs for the third ammonia molecules bound to Ti^+, Cr^+, Fe^+, and Co^+ and BDEs for the fourth ammonia bound to all metals but V^+ and Cu^+ are reported for the first time. In the discussion that follows, we compare our results to previous theoretical and experimental values and then provide a brief overview of the bonding in $M^+(NH_3)_x$ molecules followed by a detailed discussion of the results for all of the $M^+(NH_3)_x$ systems examined in this study. Intrinsic to this discussion is the assumption that the ammonia ligands bond directly to the metal ions rather than to other ammonia ligands in all cases, as found by calculations on the $Cu^+(NH_3)_{1-4}$ complexes.[12]

Comparison between Results of This Study and Theory. There have been two theoretical studies on $M^+(NH_3)_x$ BDEs. The $M^+(NH_3)_x$ BDEs ($x = 1, 2$) for M = Sc−Cu were calculated by LBPS[4] and the $Cu^+(NH_3)_x$ BDEs ($x = 1-4$) were computed by BLP.[12] Both theoretical studies were carried out at the MCPF level of theory and can therefore be easily compared.

The agreement between the results of this study and the results of LBPS[4] for the M^+-NH_3 BDEs is very good. This is shown visually in Figure 5. The theoretical values of LBPS average 96 ± 4% of our experimental values, and all values are within the uncertainties in the determinations. The biggest difference is 21 kJ/mol for Cu; however, the result of BLP[12] differs from the present result by only 13 kJ/mol, within the uncertainty of

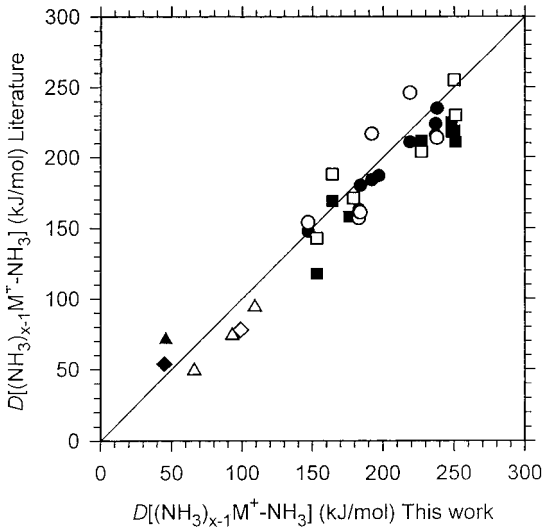

Figure 5. Results from this work versus those in the literature for 298 K binding enthalpies in kJ/mol of first-row transition metal ion−ammonia complexes $M^+(NH_3)_x$, where $x = 1$ (circles), $x = 2$ (squares), $x = 3$ (triangles), and $x = 4$ (diamonds). Open symbols show comparisons to the experimental values of Marinelli and Squires (ref 5). Closed symbols show comparisons to theoretical values (refs 4 and 12). The line has unity slope and zero intercept.

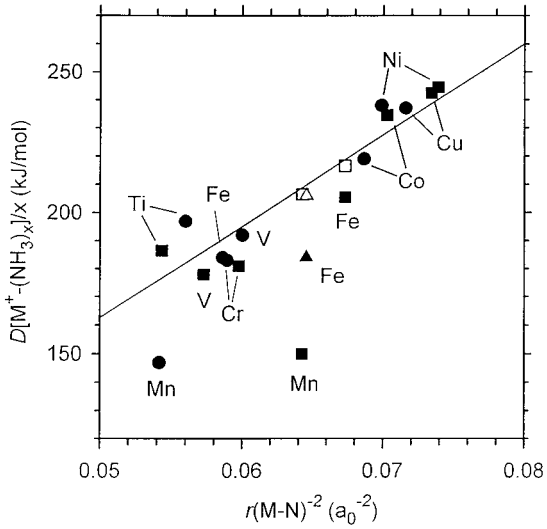

Figure 6. Metal−ammonia bond dissociation energies (in kJ/mol) at 0 K from the present work versus the inverse square of the metal−nitrogen bond distance (in bohr) calculated by LBPS (ref 4). Values for $M^+(NH_3)_x$ complexes where $x = 1$ (circles) and the average BDE for $x = 2$ (squares) are shown. The triangle shows the $Fe^+(NH_3)$ bond energy at the bond distance for the quartet (rather than sextet) state. The open symbols for Mn and Fe indicate bond energies corrected by the promotion energy as discussed in the text. The line shows a linear regression analysis with a zero intercept of all points but those for Mn.

either study. LBPS[4] do not provide an explanation for the difference in the two calculated bond energies. The excellent agreement between theory and experiment for the monoligated complexes gives us considerable confidence in the accuracy of the present values.

The overall agreement between the results of LBPS[4] and the results of this study for the $(NH_3)M^+-NH_3$ BDEs is also satisfactory, although it is not as good as for the M^+-NH_3 BDEs. The $(NH_3)M^+-NH_3$ BDEs for M = Ti,V, Cr, and Fe calculated by LBPS[4] are within the combined uncertainties of the results of this study. For all other metals studied, the present results are higher than those of LBPS.[4] Considering all eight metals studied, the theoretical numbers average 90 ± 8% of our experimental values for the second ammonia ligand. This is consistent with the observation of these authors that their bond energies may be too low due to "limitations in the one particle basis sets and an underestimation of the correlation contribution to the binding energies at the MCPF level of theory". Overall, these results may suggest that the theoretical calculations have underestimated the effects of 4s−3d σ hybridization on the second ligand binding energy, as first suggested by BLP in their study of $Cu^+(NH_3)_x$ BDEs.[12] Indeed, although their calculations found the 0 K BDE for $Cu^+(NH_3)$ was greater than that for $Cu^+(NH_3)_2$, they suggested that the second ammonia BDE was probably greater than the first. The results of this study verify that prediction.

The study of LBPS[4] typically finds more negative values for the differences between the second and first ammonia bond energies, $\Delta(2,1) = D[(NH_3)M^+-NH_3] - D[M^+-NH_3]$, than is determined in this study (Table 4). In the cases of Mn and Ni, this leads to a change in sign for the $\Delta(2,1)$ value when theory and experiment are compared. In this regard, we note that the relative values for these bond energies obtained by Marinelli and Squires[5] agree with the present results for Ni and are within experiment error for Mn. LBPS[4] noted that their second bond energy to Mn^+ could be low by as much as 25 kJ/mol because proper treatment of 4s−3d interactions is particularly critical to the bonding. The only exceptions to the observation that our values of $\Delta(2,1)$ are more positive than $\Delta(2,1)$ values determined by LBPS[4] are the cases of Cr and V. In these cases, theory and experiment agree within the uncertainties.

The only previous theoretical study of triply and quadruply ligated systems is the study of $Cu^+(NH_3)_3$ and $Cu^+(NH_3)_4$ by BLP.[12] As found in the experimental studies, BLP[12] determined that the third and fourth ammonia BDEs were drastically less than the first two. BLP[12] calculated the $Cu^+(NH_3)_3$ BDE to be 71 ± 13 kJ/mol, 25 ± 14 kJ/mol higher than the present result. For the $(NH_3)_3Cu^+-NH_3$ BDE, BLP[12] report a value of 54 ± 13 kJ/mol, in good agreement with the value of 45 ± 6 kJ/mol determined here.

One means used by LBPS[4] to evaluate their bond energies was to recognize that largely electrostatic bonds should have BDEs approximately proportional to $1/r(M-N)^2$. They obtained a reasonably linear relationship when their D_0 values were plotted vs their calculated $1/r(M-N)^2$ values. A similar plot of the present BDE values, $D_0(M^+-NH_3)$ and $\{D_0(M^+-NH_3) + D_0[(NH_3)M^+-NH_3]\}/2$, is shown in Figure 6. We use the average of the first and second BDEs to describe the $M^+(NH_3)_2$ complexes rather than $D_0[(NH_3)M^+-NH_3]$, as LBPS[4] did, because this implicitly recognizes that the two M−N bonds in the $M^+(NH_3)_2$ complexes are equivalent, i.e. they have the same bond lengths. It is only the electronic reorganization accompanying the loss of one ligand to form $M^+(NH_3)$ that distinguishes these two bond energies. The excellent correlation obtained with the inverse square of the calculated bond distances for both the first BDE and the average of the first two BDEs suggests that this choice is a reasonable one.

The clear exceptions to this correlation are the values for Mn, which fall well below the other values. This was also observed by LBPS,[4] who noted that the binding energy of $Mn^+(NH_3)_2$ is an exceptional case as it correlates with a highly excited state of Mn^+, as discussed further below. We believe that the $Mn^+(NH_3)$ value may also be an exception because it involves a different bonding mechanism from most of the other metals, as discussed below.

Comparison to Previous Experimental Results. There are only two previous experimental studies on the BDEs of $M^+(NH_3)_x$ molecules. Holland and Castleman conducted equilibrium measurements of the $(NH_3)Cu^+-NH_3$ and $(NH_3)_2Cu^+-NH_3$ BDEs.[10] Early CID experiments were used by Marinelli and Squires (MS)[5] to measure the $(NH_3)_{x-1}M^+-NH_3$ ($x = 1$, 2) BDEs for M = V−Ni, the $(NH_3)_2M^+-NH_3$ BDEs for M = V, Mn, and Ni, and the $(NH_3)_3V^+-NH_3$ BDE. These results are summarized alongside the results of this study in Table 4.

Figure 5 shows that the experimental results of MS[5] for the first and second metal ion−ammonia bond energies have the same general magnitude and trends as the present data. The results of MS[5] and the present study are within combined experimental uncertainties for all M^+-NH_3 and $(NH_3)M^+-NH_3$ BDEs jointly studied. However, specific values can differ appreciably from the present results, e.g. V^+-NH_3 and Co^+-NH_3 BDEs from MS[5] (the two systems identified by LBPS as suspect) are higher than the results of this study by 25 and 27 kJ/mol, respectively, while those of Cr^+-NH_3, Fe^+-NH_3, and Ni^+-NH_3 are lower by 26, 23, and 24 kJ/mol, respectively. In this regard, it might be remembered that the work of MS[5] is a fairly early CID study performed before some of the details necessary for acquiring the most accurate thermochemistry had been established.

The relative values of the first and second ammonia bond energies determined here and by MS[5] are in much better agreement. These experimental values for $\Delta(2,1)$ are quite close in all cases but Cr, Mn, and Co, although these values are still well within the experimental uncertainties. In the cases of Cr and Mn, the sign of $\Delta(2,1)$ determined here and by MS[5] differ, although the magnitude of $\Delta(2,1)$ is small in both cases. We believe that the value for the Cr^+-NH_3 BDE determined by MS[5] is suspect because it is only 3 kJ/mol greater than the value determined for the Mn^+-NH_3 BDE. In previous studies of transition metal ion−ligand systems,[1,2] the first Mn^+−ligand BDE was observed to be significantly less than the first metal ion−ligand BDE for all other first-row transition metals.

The study of MS[5] measured the $(NH_3)_2M^+-NH_3$ BDEs for only M = V, Mn, and Ni and the $(NH_3)_3M^+-NH_3$ BDE for only M = V. As in the present work, MS[5] find that these BDEs are significantly lower than the M^+-NH_3 and $(NH_3)M^+-NH_3$ BDEs. Figure 5 and Table 4 shows that the third and fourth BDEs measured by MS are systematically lower than the analogous values determined here, by 15−20 kJ/mol. We believe that this is largely a consequence of neglecting the internal energy in their threshold analysis. The average vibrational energies of the $M(NH_3)_3^+$ and $M(NH_3)_4^+$ complexes at room temperature are 0.23 ± 0.03 and 0.31 ± 0.04 eV (22 and 30 kJ/mol), comparable to the discrepancies observed.

The equilibrium study of HC[10] determined that the third and fourth Cu^+−ammonia BDEs are 59 and 54 kJ/mol. Uncertainties representing the reproducibility of these values (but not systematic errors) are 1 kJ/mol. The differences between the values determined by HC[10] and in the present study are comparable to those observed for the BDEs of $Cu(H_2O)_3^+$ and $Cu(H_2O)_4^+$ determined by HC[10] and in a previous CID study from our laboratories.[3] Overall, the agreement seems reasonable given the very different methods used to ascertain the thermochemistry. We also note that both experimental studies find that the third and fourth ammonia BDEs to Cu^+ are similar to one another, in contrast to the theoretical results which give a much larger third BDE.

Overview of Transition Metal Ion−Ligand Bonding. In this overview, we summarize the findings of theoretical calculations[4,12] concerning the bonding of ammonia to transition metal ions and other factors that have been found to be influential in the bonding of metal−ligand complexes. This bonding is controlled by a balance between ion−dipole attraction and Pauli repulsion between the metal and the ligand. The electrostatic contribution to the bonding increases from left to right across the periodic table as the ionic radius of the metal decreases. Transition metals have three primary mechanisms for decreasing Pauli repulsion between the metal and ligand: 4s−4p polarization, 4s−3d σ hybridization, and promotion to a more favorable electronic state. 4s−4p polarization is more energetic than 4s−3d σ hybridization because the 4p orbitals are higher lying.[33] This mechanism allows electron density to polarize to the opposite side of the metal away from the ligand, thereby allowing the ligand to feel a larger effective nuclear charge. 4s−4p polarization can be effective for singly ligated systems, but for doubly ligated systems, electrons in the 4s−4p hybrid orbital behave as a third ligand forcing the complex into a geometry with a small ligand−metal−ligand bond angle and larger ligand−ligand repulsions.[4,33] 4s−3d σ hybridization is often a more effective way to reduce metal−ligand repulsion for doubly ligated systems. The 4s−3d σ hybridization scheme forms an orbital which places electron density in a direction perpendicular to the bonding axis. This allows both the first and second ligands to see a higher effective nuclear charge.[33] For 4s−3d σ hybridization to occur, the transition metal center must exist in a state that is a combination of a $4s^13d^n$ configuration and a $3d^{n+1}$ configuration. Thus, for metals having a $4s^13d^n$ ground configuration, one must consider the promotion energy required to achieve a $3d^{n+1}$ configuration. For metals having a $3d^{n+1}$ ground configuration, one must consider the promotion energy required to achieve a $4s^13d^n$ configuration. The primary consequence of 4s−3d σ hybridization is that the second metal−ligand BDE can be greater than the first BDE because the energetic cost of hybridization is primarily paid by the first ligand. For triply and quadruply ligated systems, there is typically a large decrease in BDE relative to the singly and doubly ligated systems, and this is also observed for the ammonia systems (Figure 7). This is a result of increased ligand-ligand repulsion and the loss of 4s−3d σ hybridization mechanisms for reducing Pauli repulsion.[12] The latter occurs because the symmetry of the 4s−3d σ hybrids are effective for only two ligands on opposite sides of the metal. BLP estimate that ligand−ligand repulsion is the larger of the two effects in the case of copper ion−ammonia complexes.[12]

In addition to these hybridization effects, one can also consider the role of promoting to an electronically excited state. In addition to the configuration interaction of $3d^{n+1}$ and $4s^13d^n$ states having the same spin, as noted above, one can also observe the thermodynamic consequences of changing spin state to optimize transition metal−ligand bonding. One simple case where such a spin change is likely occurs when interaction of $3d^{n+1}$ and $4s^13d^n$ configurations necessary for 4s−3d σ hybridization is not possible (e.g., there are no $3d^{n+1}$ states having the same spin as high spin coupled $4s^13d^n$ states when $n \geq 5$). Promotion to a state of lower spin is required before the hybridization mechanism discussed above is possible. Another way of viewing such a promotion is to note that as ligands are placed around the metal, the degeneracy of the metal d orbitals is split according to the symmetry of the ligand field. As more ligands are added, the strength of the field increases and the splitting between orbitals increases. Eventually, it is possible

(33) Bauschlicher, C. W.; Langhoff, S. R.; Partridge, H. In *Organometallic Ion Chemistry*; Kluwer Academic Publishers: Dordrecht, The Netherlands, 1996.

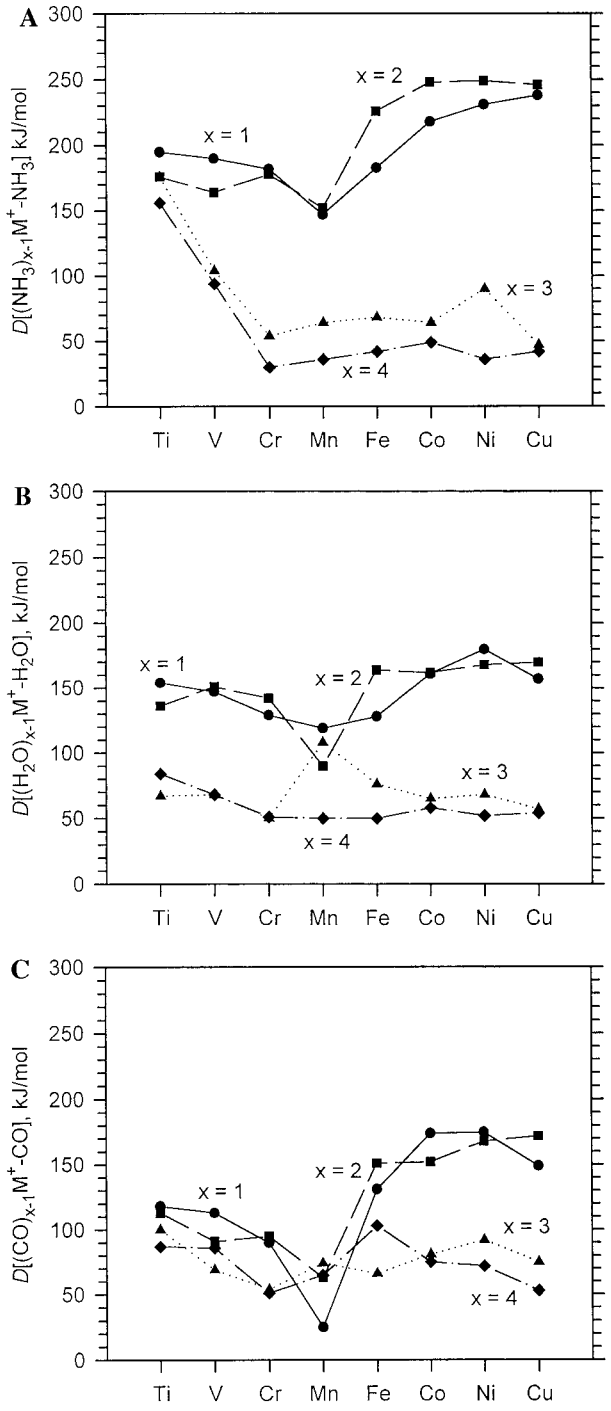

Figure 7. Periodic trends in the 0 K bond energies in kJ/mol of first-row transition metal ion−ligand complexes for one (circles), two (squares), three (triangles), and four (diamonds) ammonia (a), water (b), and carbonyl (c) ligands.

that the difference in orbital energies becomes greater than the stabilization derived from exchange interactions and the metal−ligand complex adopts a lower spin state. When this occurs, electrons are removed from high-lying orbitals with antibonding character and put into orbitals with bonding character, potentially resulting in a higher BDE.[1,2]

In the discussions of the results for the individual transition metal ions which follow below, the trends in BDEs shown in Figure 7 will be discussed in terms of the concepts described above. We start with the metals to the right of the periodic table as these can be understood most easily in simple electrostatic terms.

Copper, Nickel, and Cobalt. Both the first and second ammonia BDEs to Cu^+, Ni^+, and Co^+ are observed to be fairly high (Table 4 and Figure 7). This is a consequence of two features of these metals. First, there is a strong electrostatic contribution to the bonding for the late first-row transition metal ions because they have small ionic radii relative to the earlier transition metals. Small changes in the ionic radii of the metal ions qualitatively explain the increase in bonding from Co^+ to Cu^+, as illustrated in Figure 6. Second, the electronic ground states of the metal ions are all $3d^n$. As a result, there is no metal−ligand repulsion resulting from occupation of the metal 4s orbital. This shortens the M−N bond length and leads to a stronger electrostatic interaction.[4] The ammonia complexes of Co^+, Ni^+, and Cu^+ are calculated to have triplet, doublet, and singlet ground states,[4,12] respectively, matching the $Co^+(^3F, 3d^8)$, $Ni^+(^2D, 3d^9)$, and $Cu^+(^1S, 3d^{10})$ atomic ion ground states.

The $(NH_3)M^+-NH_3$ BDEs for M = Co, Ni, and Cu are greater than the M^+-NH_3 BDEs by 10−30 kJ/mol because the binding of the first ammonia ligand pays much of the cost of 4s−3d σ hybridization. The BDEs for the third and fourth ammonia molecules decrease dramatically. This is a result of increased ligand−ligand repulsion and the loss of 4s−3d σ hybridization that reduces metal−ligand repulsion.

Although the BDEs for the third and fourth ammonia molecules are small relative to the BDEs for the first and second ammonia ligands, the $(NH_3)_2Ni^+-NH_3$ BDE is 20−50 kJ/mol greater than the $(NH_3)_2M^+-NH_3$ BDE observed for the other late first-row transition metals. This result seems somewhat anomalous, although we note that our bond energy is consistent with that measured by MS[5] once the effect of internal energy is properly accounted for (see discussion above). This high BDE cannot be justified in terms of a change in spin state because all nickel ion ammonia complexes are expected to correlate with the ^2D ($3d^9$) ground state of nickel.[4] We also note that the relative BDEs of other triply ligated Ni^+ complexes are slightly larger than those of Co^+ and Cu^+ complexes, e.g. where the ligand is H_2O[3] or CO,[34−36] although the magnitude of the difference is less in these other systems. Further, the fourth nickel−ammonia bond energy is weaker than those of Co and Cu, consistent with the result expected for a stabilized $Ni^+(NH_3)_3$ complex. This result is particularly significant when it is realized that all bond energies measured by CID are completely independent measurements that do not rely on the thermochemistry of smaller complexes. An explanation for this enhanced BDE is not immediately evident, although it is apparently common to many ligand systems.

Iron. The Fe^+-NH_3 BDE is less than the Co^+-NH_3 BDE by 35 kJ/mol. This result is in line with the steady decrease in M^+-NH_3 BDEs from Cu^+ to Mn^+ (Figure 6). The Fe^+-NH_3 bond length is calculated to be much longer than those for Co−Cu, which is primarily because the ground state of this complex is ^6E, correlating with the $^6D(4s^13d^6)$ ground state of Fe^+. This high-spin state cannot utilize 4s−3d σ hybridization to enhance the bonding, but rather uses 4s−4p polarization. LBPS[4] calculate that the $^4A_2$ state correlating with the $^4F(3d^7)$ excited state of Fe^+ lies 0.22 eV higher in energy, an excitation energy comparable to the $^6D-^4F$ excitation energy for the atomic iron cation, 0.248 eV.[37]

(34) Meyer, F.; Chen, Y.-M.; Armentrout, P. B. *J. Am. Chem. Soc.* **1995**, *117*, 4071.
(35) Khan, F. A.; Steele, D. L.; Armentrout, P. B. *J. Phys. Chem.* **1995**, *99*, 7819.
(36) Goebel, S.; Haynes, C. L.; Khan, F. A.; Armentrout, P. B. *J. Am. Chem. Soc.* **1995**, *117*, 6994.

Although the calculations indicate that the ground state of $Fe^+(NH_3)$ is ^6E and there is good agreement between the calculated and experimental BDEs, it does seem surprising that the BDE of ammonia to $Fe^+(4s^13d^6)$ is so much greater than to $Mn^+(4s^13d^5)$, see below. Therefore, we also consider whether our data might be more consistent with a quartet ground state for this complex. Binding to the ^4F state of Fe^+ is advantageous because this state can utilize 4s−3d σ hybridization to reduce the Pauli repulsion, similar to that of Co−Cu. A simple prediction of the BDE for this state would be that of $Co^+(NH_3)$ reduced by the promotion energy of 0.248 eV and by a lower electrostatic interaction resulting from the larger ion size. On the basis of bond lengths calculated for $Co^+(NH_3)$ and $Fe^+(NH_3)$ ($^4A_2$) by LBPS and the correlation shown in Figure 6, this latter effect is about 13 kJ/mol, such that the estimated BDE of $Fe^+(NH_3)$ in its quartet state is about 182 kJ/mol (=219−24−13), in good agreement with our measured value. However, this value does not agree well with the 298 K BDE actually calculated by LBPS for the $^4A_2$ state, 159 kJ/mol, although this point is well within the scatter of the data shown in Figure 5. Another way to consider whether a quartet might be the correct ground state is to examine the correlation with bond distance (Figure 6). This point, shown by the triangle, falls off the correlation shown; however, this BDE should be increased by the $^6D-^4F$ excitation energy to correctly correlate to the atomic state used to generate this complex. This point, indicated by the open triangle, agrees nicely with the correlation obtained from the other metals. Hence, the experimental data appear to be consistent with either a sextet or quartet ground state for the $Fe^+(NH_3)$ complex and cannot be used for an unambiguous assignment.

The $(NH_3)Fe^+-NH_3$ BDE is 43 kJ/mol greater than the $Fe^+(NH_3)$ BDE, a greater increase than observed for any other first-row transition metal ion. Both MS[5] and LBPS[4] obtained a similar result, which is comparable to that observed previously for $Fe^+(H_2O)_2$.[3] If the ground state of $Fe^+(NH_3)$ is ^6E, this observation has been attributed to two factors. First, as noted above, 4s−4p polarization is no longer an effective mechanism for reducing the Pauli repulsion between two ligands and the 4s electron; hence, the sextet state of $Fe^+(NH_3)_2$ is destabilized. Instead, LBPS[4] find that this molecule has a ^4E_g ground state that correlates to the Fe^+ (^4F, $3d^7$) excited state. Promotion to this low-spin state now allows efficient 4s−3d σ hybridization similar to that for Co−Cu. Second, the cost of the 4s−3d σ hybridization and promotion to the quartet state is largely paid by the first ligand. If the ground state of $Fe^+(NH_3)$ is $^4A_2$, the second effect is sufficient to explain the observed result. This can be estimated by noting that the increase in BDEs from the first to the second ligand for Co−Cu is 20 ± 10 kJ/mol, but this is for a spin-allowed dissociation. Hence, we expect that the $(NH_3)Fe^+-NH_3$ BDE should exceed the first including a 24 kJ/mol correction for the $^6D-^4F$ excitation energy, namely (184 ± 12) + 24 + (20 ± 10) = 228 ± 16 kJ/mol in agreement with our measured value.

If the ground state of $Fe^+(NH_3)$ is ^6E, then we also need to discuss whether the experimental BDE measured for $Fe^+(NH_3)_2$ is an adiabatic bond energy connecting the ^4E_g ground state of this complex with the ground state of the CID products, $Fe^+(NH_3)$ (^6E) + NH_3 ($^1A_1$), or whether it is a diabatic bond energy measuring the dissociation to the spin-allowed products, $Fe^+(NH_3)$ ($^4A_2$) + NH_3 ($^1A_1$). (If the ground state of $Fe^+(NH_3)$ is $^4A_2$, then dissociation of $Fe^+(NH_3)_2$ is spin-allowed, and as discussed above, dissociation of $Fe^+(NH_3)$ must be to Fe^+ (^6D) + NH_3 ($^1A_1$) to match the correlation in Figure 6.) Experimentally, this is difficult to assess, especially because the excitation energy is fairly small in this case. (It can be accomplished if different thresholds, diabatic and adiabatic, are obtained for different CID target gases.) The correlation shown in Figure 6 again provides some insight into this question. If dissociation is adiabatic, then the sum of the bonds in $Fe^+(NH_3)_2$ should be increased by the $^6D-^4F$ excitation energy to correctly correlate to the atomic state used to generate this complex. This correction is shown by the open square in Figure 6. (This correction is also needed if $Fe^+(NH_3)$ has a $^4A_2$ ground state.) In contrast, if the bond energy measured is diabatic, then the promotion energy correction is largely included in the bond energies measured. (Actually, the excitation energy of the $Fe^+(NH_3)$ species rather than of Fe^+ is included in the measured BDEs, but LBPS[4] find that these differ by only 0.03 eV.) As the adjusted point (open square) correlates slightly better with the other bond energies than the uncorrected point (closed square), there is some evidence that the bond energy for $(NH_3)Fe^+-NH_3$ in Table 4 is the adiabatic BDE. This argument is even more convincing in the case of Mn (see below), where the same conclusion is drawn.

Upon binding a third and fourth ammonia ligand to Fe^+, the BDEs decrease dramatically in accord with the behavior of the complexes of Co^+, Ni^+, and Cu^+.

Manganese. The Mn^+-NH_3 BDE is lower than for any other transition metal ion, similar to observations for both CO[1,2] and H_2O[3] ligands. The low BDE has been attributed to the especially stable $4s^13d^5$ electronic configuration of ground-state Mn^+ (^7S). Because both the 4s and 3d σ orbitals are occupied and high-spin coupled, there is severe metal−ligand repulsion leading to a low BDE. Further, 4s−3d σ hybridization is impossible from such a high-spin state. Such hybridization would require promotion to a quintet electronic state, but the lowest energy quintet state, the $^5S(4s^13d^5)$, is 1.174 eV above the ground state.[37] Overall, this low bond energy is consistent with the $^7A_1$ ground state for $Mn^+(NH_3)$ calculated by LBPS.[4]

If the second NH_3 ligand were to bind to Mn^+ (^7S), we should observe a decrease in the BDE because of the ineffectiveness of 4s−4p polarization for two ligands. Indeed, for $Mn^+(H_2O)_2$, which has a septet ground state,[12] the second ligand is bound by 0.30 eV less than the first.[3] Instead, we find that the second ammonia bond is comparable to the first, although it is still lower than any other $(NH_3)M^+-NH_3$ BDE. The lack of a considerable decrease in BDE on going from one to two ligands indicates that the spin changes from a septet to quintet upon binding the second ammonia. This is consistent with results from the theoretical study of LBPS,[4] where it was determined that that the lowest energy state of $Mn^+(NH_3)_2$ is $^5A_{1g}$, derived from a mixture of $^5S(4s^13d^5)$ and $^5D(3d^6)$ metal electronic configurations. Thus, the low second Mn^+ BDE is a consequence of the high promotion energy necessary to put the Mn^+ into the correct asymptotic state.

As in the case of $Fe^+(NH_3)_2$, we need to consider whether ground-state $Mn^+(NH_3)_2$ ($^5A_{1g}$) dissociates diabatically (spin-conserving) or adiabatically (spin-changing) to $Mn^+(NH_3)$ + NH_3. As in the iron case, we examine the correlation in Figure 6 and correct the sum of the first two bond energies by the excitation energy to the ^5S state at 1.174 eV (use of the excitation energy to the ^5D state at 1.808 eV puts the calculated value 30 kJ/mol higher). Clearly, the original data point does not correlate with the other metals, while the data adjusted for the ^5S promotion energy are in good agreement. In this case,

(37) Moore, C. E. *Atomic Energy Levels*; U.S. National Bureau of Standards: Washington, DC, 1952; Circ. 467. Sugar, J.; Corliss, C. *J. Phys. Chem. Ref. Data*, **1981**, *10*, 197, 1097; **1982**, *11*, 135.

there is little ambiguity that the BDE measured by CID corresponds to the adiabatic value, a result that is also likely for $Fe^+(NH_3)_2$.

As in the case of the previously discussed transition metals, the BDEs for the third and fourth ammonia molecules are much smaller than the BDEs for the first and second ammonia molecules. This is a consequence of increasing ligand−ligand repulsion and loss of mechanisms for reducing Pauli repulsion.

Chromium. The Cr^+-NH_3 BDE is greater than the Mn^+-NH_3 BDE because the 4s orbital is unoccupied in Cr^+. This leads to reduced metal−ligand repulsion and a smaller M^+-N bond length. However, the $^6S(3d^5)$ configuration of Cr^+ requires that the 3d σ orbital be occupied. This increases the metal−ligand repulsion leading to weaker BDEs than observed for Ti^+ and V^+ (discussed below). Some reduction in this repulsion can be realized by 4s−3d σ hybridization. The $(NH_3)Cr^+-NH_3$ BDE is observed to be comparable to the Cr^+-NH_3 BDE. Apparently, the 4s−3d σ hybridization is not as influential as for the later transition metals, such that no strong enhancement in the second BDE is observed.

As for the late first-row transition metal ions, the BDEs for the third and fourth decrease dramatically because of the loss of mechanisms for decreasing Pauli repulsion and increasing ligand−ligand repulsion.

Vanadium. The first and second vanadium ion bond energies to ammonia are weak compared to the late transition metal ions. This is simply because of the larger radial extent of the vanadium ion compared to these species, as can be seen from Figure 6. LBPS[4] calculate that both $V^+(NH_3)$ and $V^+(NH_3)_2$ have quintet ground states that correlate with the V^+ (^5D, $3d^4$) ground state. The calculations of LBPS indicate appreciable 4s electron density (suggesting 4s−3d σ hybridization), but a reviewer suggests that this may be largely electron density donated by the ligands. If 4s−3d σ hybridization is present, it clearly does not have the effect of allowing the second ammonia binding energy to be greater than the first, which seems counterintuitive given that 4s−3d σ hybridization is supposed to be more efficient for the early metals.[33] Presumably, 4s−3d σ hybridization is a relatively unimportant mechanism for reducing Pauli repulsion by this early transition metal because both the 4s and 3d σ orbitals can be empty in a $3d^4$ configuration. Thus, ligand−ligand repulsions become more influential in the trends for the sequential metal−ligand BDEs leading to gradually declining values.

The $(NH_3)_2V^+-NH_3$ BDE is high relative to the $(NH_3)_2M^+-NH_3$ BDEs observed for the late transition metals. However, there is still a decrease of 55 kJ/mol between the $(NH_3)V^+-NH_3$ and $(NH_3)_2V^+-NH_3$ BDEs. Theory predicts the ground state of $V^+(NH_3)_2$ to be a quintet, and the significant decrease in BDE indicates that the spin probably does not change upon binding a third ammonia. The high $(NH_3)_2V^+-NH_3$ BDE is probably a result of the fact that the vanadium monocation only has four valence electrons and does not need to occupy destabilizing orbitals to the same extent as in the late transition metals.

The $(NH_3)_3V^+-NH_3$ BDE is only slightly smaller than the $(NH_3)_2V^+-NH_3$ BDE. As for the third bond energy, this BDE would appear to be stronger than the later transition metals primarily because antibonding 3d orbitals are not occupied. It is also possible that a spin change to a triplet state occurs upon addition of the fourth ammonia ligand.

Titanium. The bond energies of $Ti^+(NH_3)$ and $Ti^+(NH_3)_2$ are slightly higher than those of the analogous vanadium system. This seems understandable from the point of view that the extra electron held by vanadium goes into antibonding orbitals of the complex. However, the correlation with $r(M-N)^{-2}$ (Figure 6) shows that the Ti complexes would be expected to be slightly weaker than the V complexes if the bonding is exclusively electrostatic. The observation that the Ti BDEs lie slightly above the correlation may indicate a higher degree of covalent interaction than metals farther to the right. The second titanium−ammonia BDE is weaker than the first, for the same reasons offered above for vanadium.

Of particular interest here is that the $(NH_3)_2Ti^+-NH_3$ BDE is comparable to the $(NH_3)Ti^+-NH_3$ BDE, rather than being weaker as in the case of vanadium and chromium. Theory predicts the ground state of $Ti^+(NH_3)_2$ to be a quartet,[4] unchanged from the ground state of the atomic metal ion. It is possible that the high $(NH_3)_2Ti^+-NH_3$ BDE is a result of the spin changing from a quartet to a doublet upon binding the third ammonia. Ti^+ has low-lying $^2F(4s^13d^2)$ and $^2G(3d^3)$ states only 0.56 and 1.09 eV above the ground state.[37] A doublet spin allows all three metal electrons to be placed in the lowest orbitals (the *xz* and *yz* orbitals in a trigonal planar ligand field) removing one from a more antibonding orbital. This postulate is similar to the spin change invoked by Dalleska et al.[3] to explain the observation that the $(H_2O)_3Ti^+-H_2O$ bond is stronger than $(H_2O)_2Ti^+-H_2O$. Because NH_3 is a stronger field ligand than H_2O, it is reasonable for a spin change to take place upon the addition of only three ammonia molecules, compared to four water ligands.

Another interesting result is that the $(NH_3)_3Ti^+-NH_3$ BDE is much larger than any other $(NH_3)_3M^+-NH_3$ BDE. If one assumes a tetrahedral geometry for $Ti^+(NH_3)_4$, this result can be interpreted as follows. If $Ti^+(NH_3)_3$ is a doublet, then it is likely that $Ti^+(NH_3)_4$ is also a doublet. In a tetrahedral ligand field, there are two low-lying 3d orbitals and three antibonding 3d orbitals. A titanium monocation complex can accommodate all three of its valence electrons in the low-lying 3d orbitals if it has a doublet spin state. Vanadium, which has a ^5D ($3d^4$) ground state, would have to have a singlet spin state to place all of its electrons in the low-lying 3d orbitals. The later transition metal monacations, having five or more valence electrons, must occupy at least one of the destabilizing orbitals.

An alternate but related explanation of the anomalous third bond energy observed for titanium−ammonia complexes involves σ bond activation. Van Koppen et al.[38] have observed evidence that the $Ti^+(CH_4)_3$ complex spontaneously activates a C−H bond to rearrange to $(CH_4)_2Ti^+(H)(CH_3)$. Because of a barrier between these species, an equilibrium mixture of the two is apparently established. This C−H activation process relies on ligation stabilizing the doublet state of Ti^+, which reacts efficiently with methane at thermal energies.[39] Although the N−H bond of ammonia is stronger than the C−H bond of methane, the binding energies of ammonia and NH_2 to Ti^+ are stronger than those of methane and CH_3.[1] Thus, it is certainly possible that the $TiN_3H_9^+$ species generated in our flow tube does not have the $Ti^+(NH_3)_3$ structure but rather is $(NH_3)_2Ti^+(H)(NH_2)$ and $TiN_4H_{12}^+$ is not $Ti^+(NH_3)_4$ but $(NH_3)_3Ti^+(H)(NH_2)$. Formation of covalent Ti−H and $Ti-NH_2$ bonds places the Ti^+ in a doublet spin state which could enhance the bonding of the remaining ammonia ligands by emptying nonbonding 3d orbitals. The presence of such isomers could have been detected by observing products such as $(NH_3)_xTi^+(H)$ and $(NH_3)_xTi^+(NH_2)$. No evidence for such products was observed, although

(38) Van Koppen, P. A. M.; Kemper, P. R.; Bushnell, J. E.; Bowers, M. T. *J. Am. Chem. Soc.* **1995**, *117*, 2098.

(39) Sunderlin, L. S.; Armentrout, P. B. *J. Phys. Chem.* **1988**, *92*, 1209.

the observation of these products would be difficult. This is because the Ti−H and Ti−NH_2 covalent bonds are stronger than the Ti−NH_3 dative bonds, such that these products would be formed less efficiently and at higher energies than dissociation of intact NH_3 molecules.

Periodic Trends and a Comparison with Other First-Row Transition Metal Ion−Ligand Systems. The periodic trends in the first-row transition metal ion−ammonia bond energies are shown in Figure 7a, while Figure 7b,c illustrates these trends for the analogous water[1] and carbonyl[1,18,19,34−36,40,41] ligand systems. There are a couple of notable differences in these patterns that provide information regarding the nature of the metal−ligand bonding in all these systems.

The most obvious difference is that the first two NH_3 BDEs are much larger than those for H_2O and CO. Compared to CO, which has a dipole moment of only 0.1 D, NH_3 bonds are stronger because its dipole moment is much higher, 1.47 D, leading to larger electrostatic interactions.[42] However, the dipole moment of water, 1.84 D, is larger than that of ammonia. Theory[4] has noted that, when discussing the electrostatic contribution to bonding, it is not sufficient to consider only the dipole moment. One must also consider the proximity of the effective dipole moment of the ligand to the transition metal center. Theoretical calculations have determined that the effective position of the ammonia dipole moment in an $M^+(NH_3)_x$ molecule is 0.48 Å closer to the transition metal than the effective position of the water dipole moment in an $M^+(H_2O)_x$ molecule,[4] thereby leading to much larger electrostatic interactions.

It is also interesting that the third and fourth metal ion−ammonia bond energies are generally weaker than those for CO complexes, although more comparable to those for the water complexes. This is presumably because the same properties that make the first two ammonia ligands bind strongly also lead to strong ligand−ligand repulsions that become increasingly important as more ligands are added to the complex. Further, in the CO case, π back-bonding interactions can enhance the bond energies.

Another obvious difference in the periodic trends of the BDEs shown in Figure 7 concerns the case of Mn. For the first Mn^+−ligand bonds, CO is exceptionally weak, while H_2O and NH_3 form moderately strong bonds. This is because the latter two ligands are polar enough to induce 4s−4p hybridization, while the nonpolar CO molecule cannot do this efficiently. For the second and third Mn^+−ligand bonds, the patterns differ for each ligand and have been explained in terms of changes in spin from a septet state that correlates with ground-state $Mn^+(^7S, 4s^13d^5)$ to a quintet state correlating with $Mn^+(^5S, 4s^13d^5)$ and $Mn^+(^5D, 3d^6)$. It has been argued that this spin change requires three H_2O but only two CO or NH_3 ligands, thereby leading to the distinct patterns in bonding for these three ligands bound to Mn^+. A similar spin change may also be occurring for Ti^+, although its consequences are less dramatic. These differences illustrate that ammonia is a fairly strong field ligand that grossly affects the energy splittings of the 3d metal orbitals.

As noted in the Introduction, one key reason for studying transition metal ammonia complexes is to examine a ligand that does not engage in substantial π interactions with the metal. The influence of this can be seen best by comparing the BDEs in $M^+(NH_3)_x$ ($x = 1, 2$) molecules to the BDEs in $M^+(CO)_x$ ($x = 1, 2$) molecules, where the ligand is a π acceptor, and the BDEs in $M^+(H_2O)_x$ ($x = 1, 2$) molecules, where the ligand is a π donor. In $M^+(NH_3)_x$ molecules, the BDEs for the late first-row transition metals (Co−Cu) are roughly 60 kJ/mol greater than for early first-row transition metals (Ti−Cr). This represents an increase in BDE of 32%. As discussed above and shown in Figure 6, this is increase is largely due to electrostatics, i.e. the late metals are smaller than the early metals. In $M^+(CO)_x$ molecules, the BDEs for the late first-row transition metals are also greater than the BDEs for the early first-row transition metals. Again the increase is roughly 60 kJ/mol, but this represents a 60% increase in BDEs. We conclude that the larger relative enhancement for the carbonyl complexes is due to the larger number of π electrons available to the late first-row transition metals for back-donation into the vacant π^* orbital of the CO.

For $M^+(H_2O)$ molecules, the BDEs in the early first-row transition metals are more similar to BDEs for the late first-row transition metals, which increase by only 20 kJ/mol or about 16%. This is due to the ability of H_2O to π donate into the vacant d orbitals of the early first-row transition metals, thereby enhancing their BDEs. For the late first-row transition metals, water can no longer act as an effective π donor because the d orbitals are occupied. Here, the loss of stabilization due to π bonding is largely compensated for by the increased electrostatic contribution to the bonding.

Acknowledgment. D.W. gratefully acknowledges Brian Griffin, Rohana Liyanage, Felician Muntean, Mary T. Rodgers, Chad Rue, and Mike Sievers for enlightening discussions and technical assistance. This work was supported by the National Science Foundation, Grant No. CHE-9530412.

Supporting Information Available: Figures showing cross sections vs energy for $M^+(NH_3)_x$ ($x = 1-4$, M = Ti−Cu) (32 pages, print/PDF). See any current masthead page for ordering information and Web access instructions.

JA973202C

(40) Sievers, M. R.; Armentrout, P. B. *J. Phys. Chem.* **1995**, *99*, 8135.
(41) Meyer, F.; Armentrout, P. B. *Mol. Phys.* **1996**, *88*, 187.
(42) Rothe, E. W.; Bernstein, R. B. *J. Chem. Phys.* **1959**, *31*, 1619.